Optical Versus Electrical Dispersion Compensation: Role of Timing Jitter

Armando Nolasco Pinto, *Member, IEEE*, José R. Ferreira da Rocha, *Member, IEEE*, Qiang Lin, and Govind P. Agrawal, *Fellow, IEEE*

***Abstract*—This paper calculates timing jitter in intensity-modulated/direct detection lightwave systems in which chromatic dispersion is compensated in the optical domain and in systems where the effects of chromatic dispersion are mitigated by means of electrical equalization at the receiver. The authors focus on a linear communication channel and derive a new expression for the timing jitter after the photodetector using frequency-domain analysis. It shows that timing jitter depends cubically on link length when dispersion is compensated in the electrical domain. In contrast, when dispersion is fully compensated optically, timing jitter depends only linearly on the link length. A new expression for the optimum timing jitter in the presence of residual dispersion is also presented.**

***Index Terms*—Communication systems, optical fiber dispersion, optical noise, timing jitter.**

I. Introduction

DISPERSION management is an essential technique for upgrading the bit rate of existing optical links to meet the increasing traffic demand [1]. In fact, for systems operating above 10 Gb/s over standard single-mode fibers, dispersion compensation is mandatory, even for metro distances. Techniques employed for dispersion compensation can be divided into two groups. The ones that process the signal after the photodetector are called electrical. In contrast, techniques that operate on the optical signal directly are termed optical. It is also possible to perform dispersion equalization at the transmitter. However, with the model used in this paper, the results obtained will be identical to those achieved with optical equalization as long as full dispersion compensation is achieved prior to photodetection. For this reason, we include this type of equalization in the optical group.

Both types of dispersion-compensation techniques (electrical and optical) have received considerable attention in recent years. In the optical domain, the use of dispersion-compensating fibers is most prevalent, although chirped fiber Bragg gratings also appear promising [1]. In the electrical domain, a transversal filter is commonly employed, and the search for a "smart" equalizer filter capable of operating at bit rates as high as 80 Gb/s is continuing [2]–[5]. The interest in electrical compensation is motivated by the possibility of integrating such a dispersion equalizer with the photodetector and other receiver components, resulting in considerable cost reduction for the whole system. Indeed, fully integrated receivers are already available commercially for 10 Gb/s channels and may soon become available for 40 Gb/s. Other advantages of the electrical techniques include the possibility of easily and dynamically tuning the amount of dispersion compensation.

In this paper, we show that electrical equalization of dispersion suffers from a fundamental limit related to the growth of timing jitter along the fiber link. In fact, we prove that the accumulation of amplified spontaneous emission (ASE) noise in combination with fiber dispersion leads to a cubic growth of timing jitter with propagation distance. Such a cubic growth was first discovered in the context of soliton systems [6], and it was thought that it was a characteristic of nonlinear communication systems. Later work revealed that ASE produces considerable timing jitter even for nonsoliton systems [7]–[10].

We focus on a purely linear communication channel and derive a new expression for the variance of timing jitter after the photodetector using frequency-domain analysis. We show that the cubic dependence of timing jitter on link length cannot be avoided if the effects of dispersion are compensated in the electrical domain within the receiver. In contrast, when dispersion is fully compensated using optical techniques, timing jitter is reduced considerably because it depends only linearly on the link length.

II. Chromatic Dispersion and Intersymbol Interference

In modern lightwave communication systems, the maximum distance at a given bit rate is frequently limited by chromatic dispersion of the transmission fiber. A light pulse travelling through a fiber link is composed of many frequency components. Due to variations of the refractive index with optical frequency, different spectral components travel at different speeds and produce pulse broadening. Such pulse broadening can cause intersymbol interference at the decision circuit if tails of neighbor pulses overlap at the decision instant. When this occurs, the signal at the input of the decision circuit depends not only on the transmitted symbol, as it ideally should, but also on the presence or absence of pulses in the neighbor time slots.

Manuscript received February 21, 2005; revised July 22, 2005. This work was supported in part by the Portuguese Scientific Foundation, FCT, through the DOPTNET project (POSI/CPS/42073/2001), FEDER and POSI programs, and by the U.S. National Science Foundation under Grants ECS-0320816 and ECS-0334982.

A. N. Pinto and J. R. F. da Rocha are with the Department of Electronic and Telecommunications, University of Aveiro and Institute of Telecommunications, 3810-193 Aveiro, Portugal.

Q. Lin and G. P. Agrawal are with the Institute of Optics, University of Rochester, Rochester, NY 14627 USA.

Digital Object Identifier 10.1109/JLT.2005.860153

In the optical domain, one way to compensate for the dispersion effects is to force the optical signal through a device where spectral components that traveled faster slow down relative to other components. This process can in principle be adjusted to equalize the delay over the entire spectrum of an optical pulse, resulting in full dispersion compensation.

The situation is somewhat different when dispersion is compensated electronically. One way to eliminate intersymbol interference, even in the presence of chromatic dispersion, is to guarantee that at the decision time of a specific bit, pulses in all neighboring bit slots have zero amplitude. This is possible to realize by an electrical filter with a suitable transfer function. In a typical approach, this filter is designed such that the pulse spectrum has a specific shape (known as the raised-cosine spectrum) after the electrical equalizer. When the full width at half maximum of this pulse spectrum is equal to the bit rate, intersymbol interference vanishes, and no degradation due to pulse broadening is caused in spite of dispersion-induced pulse broadening.

However, both methods have difficulties in the presence of timing jitter. Clearly, if the pulse's arrival time is not certain and fluctuates around an expected value, it is not possible to define a set of points where pulse tail amplitude must vanish. In fact, this amplitude must vanish over a temporal band whose duration depends on the amount of timing jitter. As the jitter grows, this band also grows, leading eventually to a situation where the receiver cannot work properly. For this reason, it is extremely important to control the magnitude of timing jitter.

As discussed in the next section, if fiber dispersion is not fully compensated optically, pulses arriving at the receiver will have a large jitter because of its cubic growth with fiber link length. As it is unlikely that receivers employed for long-haul systems can work with such a large jitter, the ASE-induced timing jitter sets a fundamental limit on the ability to overcome the chromatic dispersion electrically. In contrast, if dispersion is compensated optically, the jitter at the receiver input is relatively small as it only grows linearly with the link length.

III. Noise Accumulation in the Frequency Domain

We consider a generic intensity-modulated/direct-detection point-to-point optical communication system. The optical transmitter launches a stream of pulses into the fiber, these pulses propagate through the fiber, being periodically amplified for fiber loss compensation, and at the system end, a receiver converts the optical pulse stream into the electrical domain and recovers the data using a decision circuit.

We consider two different types of receivers. In the first one, we force the pulse width, before the photodetector, to be the same as it was just after the transmitter. This is generically the approach followed when dispersion is compensated optically. We assume that a dispersion-compensating module (DCM) is placed just before the receiver for this purpose. In practice, many DCMs may be used all along the link. However, our use of a single DCM does not limit our conclusions, as we focus on a linear transmission system for which the place where the DCMs appear is not relevant as long as the entire accumulated dispersion is compensated such that each optical pulse recovers its original width.

In the second type of receiver, we assume that some residual dispersion is left on the link, either because DCMs are not used at all or because they are not able to fully compensate the chromatic dispersion. In this situation, optical pulses may spread over multiple time slots before the detection. Only after the photodetector, the electrical signal is shaped to guarantee that the pulse tails cross a null at all decision times other than the pulse's own decision time. This is the approach generally followed by electrical equalizers.

Random fluctuations of the pulse central position in the presence of ASE noise can occur because of two different effects: beating of signal with noise and beating of noise with noise. In this work, we focus on the jitter produced by the beating of signal with noise. We assume that the electrical equalizer is not able to eliminate the random walk of the pulse central position produced by this. As we will show, such a beating leads to a perturbation that is spectrally superimposed on the signal, thereby limiting the effect of the equalizer. However, this does not mean that the effect of the jitter on the decision circuit is independent of the electrical filter response. In fact, it is possible to tailor the filter response such that it minimizes the effect of timing jitter on the decision process (see, for instance, [11]). In this work, we focus on the optical transmission line and do not consider the optimization of the electrical filter. However, this analysis can in principle be extended to include the effect of the electrical filter.

To calculate the timing jitter, we define formally the pulse central position along the fiber link as [12]

$$t_p(z) = \frac{1}{E_p} \int_{-\infty}^{+\infty} t\,|u(z,t)|^2\,dt \tag{1}$$

where $u(z,t)$ represents the electric field envelope at position z and at time t, and the pulse energy E_p is given by

$$E_p = \int_{-\infty}^{+\infty} |u(z,t)|^2\,dt. \tag{2}$$

Because of ASE noise, t_p varies randomly from pulse to pulse, leading to timing jitter. A useful measure of this timing jitter is provided by the variance of t_p calculated using the standard definition

$$\sigma_t^2 = \overline{(t_p - \overline{t_p})^2} \tag{3}$$

where an overbar indicates an ensemble average over ASE-induced temporal fluctuations.

Equations (1) and (2) can be written in the frequency domain, using the frequency differentiation and conjugate functions theorems, and Parseval's formula [13], as

$$t_p(z) = -\frac{i}{2\pi E_p} \int_{-\infty}^{+\infty} U^*(z,\omega)\frac{\partial U(z,\omega)}{\partial \omega}\,d\omega \tag{4}$$

$$E_p = \frac{1}{2\pi}\int_{-\infty}^{+\infty} |U(z,\omega)|^2\, d\omega \tag{5}$$

where $U(z,\omega)$ is the Fourier transform of $u(z,t)$ and is defined as

$$U(z,\omega) = \int_{-\infty}^{+\infty} u(z,t)e^{i\omega t}dt. \tag{6}$$

In the absence of ASE noise, pulse propagation is completely deterministic as every pulse suffers the same propagation delay and no timing jitter occurs. Therefore, the ASE noise can be seen as the fundamental origin of timing jitter. In the case of a linear transmission system, the case studied in this paper, one can focus on a single pulse for calculating the timing jitter. However, if the transmission system is affected by fiber nonlinearities, one must consider multiple pulses simultaneously to include the additional jitter resulting from the nonlinear interaction between adjacent pulses [14].

In general, ASE noise is unpolarized as spontaneously emitted photons can have an arbitrary state of polarization. In this work, we assume that the noise component polarized orthogonally with respect to the signal is removed before photodetection. This restriction is not important as the signal only beats with the copolarized noise.

The noise added by an optical amplifier, copolarized with the signal, has the average power [15]

$$P_N = h\nu_0 n_{\rm sp} B_{\rm opt}(G-1) \tag{7}$$

where h is the Planck constant, ν_0 is the carrier frequency, $n_{\rm sp}$ is the spontaneous emission factor, $B_{\rm opt}$ is the optical bandwidth (in hertz), and G is the amplifier gain. Considering the central limit theorem, the noise added by the amplifier can be assumed to be white noise with Gaussian statistics, as discussed, for instance, in [16].

Modeling the noise as a zero-mean stationary Gaussian random process, a random fluctuation $N_k(\omega)$ is added to each frequency component of the pulse at the kth amplifier such that

$$\overline{N_k(\omega)} = 0 \tag{8}$$

$$\overline{N_k(\omega_1)N_k^*(\omega_2)} = \sigma_k^2\delta(\omega_1-\omega_2) \tag{9}$$

where σ_k^2 is the bilateral ASE noise power spectral density. Its value $\sigma_k^2 = h\nu_0 n_{\rm sp}(G-1)/2$ ensures that (7) is satisfied. Equations (8) and (9) characterize ASE noise at each amplifier output. However, to evaluate the noise at the photodetector, we must consider the effect of fiber dispersion on noise.

We are dealing with a linear transmission channel whose losses are completely compensated by optical amplifiers. However, chromatic dispersion is present and affects both signal and noise. Each fiber section between two amplifiers can be modeled as a filter with the transfer function $H(z,\omega) = \exp((i/2)\beta_2\omega^2 z + (i/6)\beta_3\omega^3 z)$, with $z = L_A$, where L_A is the amplifier spacing, and β_2 and β_3 are, respectively, the group velocity dispersion and third-order dispersion parameters of the fiber. As a result, the total noise at the end of a fiber link of length L can be written as

$$N(\omega) = \sum_{k=1}^{M} N_k(\omega)H(L-kL_A,\omega) \tag{10}$$

where M is the number of amplifiers. In (10) and hereafter, we omit the length dependence of $N(\omega)$ to simplify the notation. The first two moments of $N(\omega)$ are given by

$$\overline{N(\omega)} = 0 \tag{11}$$

$$\overline{N(\omega)N^*(\omega)} = \frac{L}{L_A}\sigma_k^2. \tag{12}$$

See Appendix A for their derivation. From (12) and the definition of σ_k^2, it follows that the bilateral ASE noise spectral density grows linearly with transmission distance L and can be written as

$$\sigma^2 = \frac{h\nu_0 n_{\rm sp}(G-1)L}{2L_A}. \tag{13}$$

IV. Timing Jitter

In this section, we use (3) to calculate the timing jitter at the photodetector. For this purpose, we replace $U(L,\omega)$ in (4) with $S(L,\omega)+N(\omega)$, where

$$S(L,\omega) = S(0,\omega)H(L,\omega) \tag{14}$$

is the spectrum of the pulse envelope in the absence of noise (it acquires a dispersion-induced phase shift due to propagation), and $N(\omega)$ is the noise spectrum at $z=L$. The pulse average position is obtained from (4) and (5) and is given by (see Appendix B for details)

$$\overline{t_p} = -\frac{i}{2\pi E_p}\int_{-\infty}^{+\infty}\left[S^*(L,\omega)\frac{\partial S(L,\omega)}{\partial\omega} + \overline{N^*(\omega)\frac{\partial N(\omega)}{\partial\omega}}\right]d\omega. \tag{15}$$

Using a similar procedure, σ_t^2 can also be calculated (see Appendix B) as

$$\sigma_t^2 = \frac{\sigma^2}{\pi E_p}T_{\rm r}^2(L) \tag{16}$$

where $T_{\rm r}(L)$ is a root-mean-square (rms) measure of the pulse width at $z=L$ and is given by

$$T_{\rm r}^2(z) = \frac{1}{E_p}\int_{-\infty}^{+\infty} t^2\,|u(z,t)|^2\,dt. \tag{17}$$

In the case of a linear communication channel with arbitrary dispersion characteristics, the rms width of a pulse can be calculated in analytic form for input pulses with arbitrary shape, width, and chirp [1, App. C]. In the case of chirp-free input

pulses of rms width $T_{\rm r} \equiv T_{\rm r}(0)$ and in a system for which the effects of β_3 are negligible, the result is found to be

$$T_{\rm r}^2(z) = T_r^2 + (\beta_2 z \sigma_\omega)^2 \tag{18}$$

where the rms spectral width of the input pulse σ_ω is obtained from

$$\sigma_\omega^2 = \frac{1}{2\pi E_p} \int_{-\infty}^{+\infty} \omega^2 \left|S(0,\omega)\right|^2 d\omega. \tag{19}$$

Equation (18) shows how chromatic dispersion along the fiber link broadens optical pulses. In the case of unchirped Gaussian pulses, $\sigma_\omega = 1/2T_r$, and we obtain

$$T_{\rm r}^2(z) = T_r^2 + \left(\frac{\beta_2 z}{2T_r}\right)^2. \tag{20}$$

This relation shows that the shortest output pulse is obtained for a specific value of input pulse width. This input pulse width is found to be [1]

$$T_{\rm r\_opt} = \sqrt{\frac{|\beta_2|L}{2}}. \tag{21}$$

Combining (16), (20), and (21), we obtain the smallest timing jitter for a given value of residual dispersion and system length

$$\sigma_{\rm t\_opt}^2 = \frac{\sigma^2}{\pi E_p} \left(|\beta_2|L\right). \tag{22}$$

V. Electrical Versus Optical Compensation of Dispersion

Equation (16) represents our main result. It shows that the variance of timing jitter after the photodetector depends on the width of optical pulses just before it. It is this width dependence that indicates that optical and electrical dispersion-compensation schemes behave quite differently as far as timing jitter is concerned.

When dispersion compensation is performed in the optical domain such that an average value of β_2 equals 0, pulses are reshaped such that their width becomes equal to its value at the fiber input. This is evident from (18), where the second term vanishes when $\beta_2 = 0$. As a result, timing jitter is given by

$$\sigma_t^2 = \frac{h\nu_0 n_{\rm sp}(G-1)}{2\pi E_p L_A} \left(T_r^2 L\right) \tag{23}$$

and it depends on the link length linearly. In contrast, when dispersion is compensated in the electrical domain, pulses are broader when they reach the photodetector and timing jitter is enhanced considerably. Using (16) and (18), we obtain for this case

$$\sigma_t^2 = \frac{h\nu_0 n_{\rm sp}(G-1)}{2\pi E_p L_A} \left[T_r^2 L + (\beta_2 \sigma_\omega)^2 L^3\right]. \tag{24}$$

The second term in this equation depends on the link length as L^3 and can be much larger than the first linear term. It is this cubic dependence that suggests electrical compensation of dispersion suffers from a major drawback related to timing jitter.

It is interesting to note that if we optimize the input pulse width for a given transmission distance L as indicated in (21), timing jitter grows only quadratically with the distance even in the presence of residual dispersion. This is easily seen by combining (13) and (22) to obtain

$$\sigma_t^2 = \frac{h\nu_0 n_{\rm sp}(G-1)|\beta_2|L^2}{2\pi E_p L_A}. \tag{25}$$

VI. Numerical Examples

It follows from (16) that the jitter resulting from beating of signal with the copolarized noise is inversely proportional to the pulse energy and can be reduced by using more energetic pulses. As the optical signal-to-noise ratio also improves with increasing pulse energy, it is important to send as much energy per pulse as possible. The values used in actual systems will be limited by the available power at the optical transmitter and by the nonlinearities of the optical channel.

In this section, we verify the accuracy of analytical expressions derived in the preceding section by solving the linear fiber propagation equation [1] using realistic system parameter values. We consider a 500-km-long lightwave system operating in the low-loss spectral window (near 1550 nm) with five ideal amplifiers ($n_{\rm sp} = 1$) spaced equally apart. The last amplifier is placed right before the optical receiver, and therefore can be considered a preamplifier. Between the preamplifier and the photodetector, an optical filter with bandwidth much larger than the pulse spectral width is placed in order to remove part of the out-of-band optical noise. We assume that the dispersion is partially compensated and a residual dispersion of 0.4 ps/nm/km was left along the link. We assume the third-order dispersion parameter [1] to be zero. Fig. 1 compares the standard deviation of pulse central position, normalized to the bit duration $T_{\rm bit} \equiv 1/B$, for three different bit rates, $B = 10$, 40, and 160 Gb/s. Unchirped Gaussian pulses with amplitude $S(0,t) = \sqrt{P_0}\exp[-t^2/(2T_0^2)]$, where P_0 is the pulse peak power and $T_0 = T_{\rm bit}/5$, were used. To estimate numerically the timing jitter, we repeated 1000 times the propagation of a single pulse with noise for each bit rate and for each distance. The average output power was kept constant at 1 mW, and the average attenuation of the fiber link, considering both the transmission and the dispersion-compensating fibers, was 0.4 dB/km.

In Fig. 1, analytical results are shown by the solid, dashed, and short dashed lines for $B = 10$, 40, and 160 Gb/s, respectively. The square symbols were obtained through numerical simulation. As it is evident, there is good agreement between the numerical and analytical results. Fig. 1 shows how timing jitter grows with the link length and the bit rate. Assuming that the system can tolerate a timing jitter up to 10% of the bit slot, which is a realistic value (see, for instance, [18]), we find that the systems operating at 10 and 40 Gb/s can, in principle, reach the 500-km mark. However, timing jitter limits the reach of the 160 Gb/s to roughly 100 km.

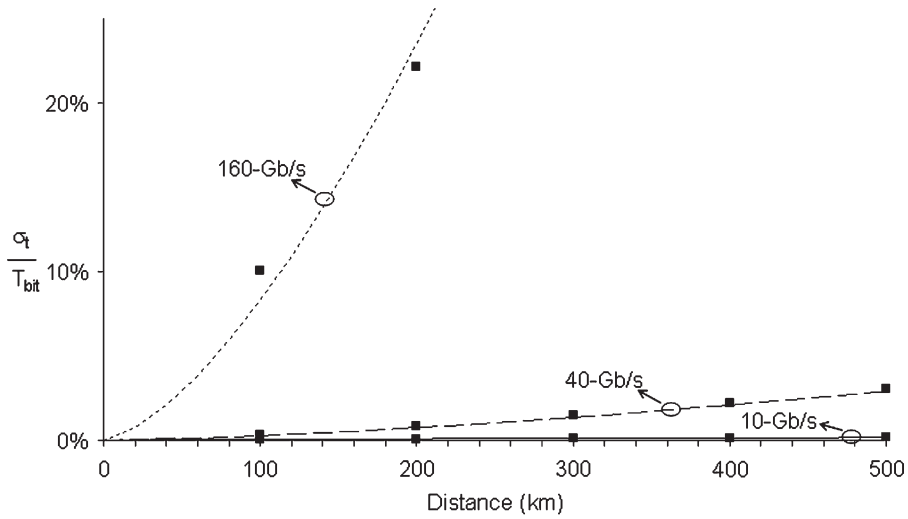

Fig. 1. Normalized timing jitter versus link length for three different bit rates (10, 40, and 160 Gb/s). Lines show analytical results; numerical results are indicated by square symbols. Values of system parameters are given in the text.

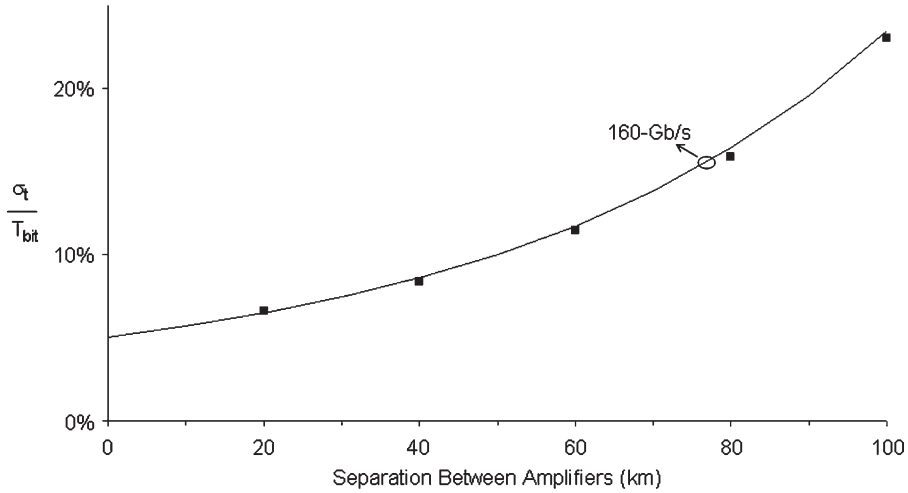

Fig. 2. Normalized timing jitter versus amplifier spacing for a 200-km-long system operating at 160 Gb/s. The solid line shows the analytical result while square symbols represent values obtained numerically.

We have also verified that timing jitter gets worse as the span length between two neighboring amplifiers increases simply because the amplifier gain increases exponentially with the span length. This is ultimately a consequence of the excess noise added to the signal. For a 200-km system, with the same parameters as the one previously considered, Fig. 2 shows the normalized timing jitter as a function of the amplifier spacing when the bit rate is 160 Gb/s. As seen there, for a 200-km system with 0.4 ps/nm/km of residual dispersion, amplifier spacing should be below 50 km to maintain timing jitter below 10% of the bit slot.

Another issue to consider is the dependence of timing jitter on system length. This dependence is linear if the chromatic dispersion is fully compensated, but becomes cubical if some residual dispersion is left within the link. In Fig. 3, we show by a short dashed line the results for a 200-km lightwave system operating at 160 Gb/s, with 100 km of span between optical amplifiers, assuming that a residual dispersion of 0.4 ps/nm/km exists along the fiber link and is compensated only after the photodetector with some kind of electrical filtering. For comparison, we also present the results obtained when the pulse width is optimized to the value $T_{\mathrm{r\_opt}}$, as indicated in (21), for each distance (long dashed curve). The case of full optical dispersion compensation is shown by a solid line. As it is evident from these results, if full optical chromatic dispersion compensation cannot be achieved in practice, the optimization of pulse width can still improve the system performance substantially.

Another interesting issue is to study how timing jitter depends on the pulse width. In the case of full dispersion compensation, timing jitter improves when pulses get shorter. A completely different situation occurs in soliton systems for which timing jitter improves when pulse width increases, leading to a tradeoff between the optical signal-to-noise ratio and the timing jitter (see, for instance, [17]).

If chromatic dispersion is mitigated electrically, the optimum pulse width is given by (21). Considering the same 500-km-long system operating at 10 Gb/s, we show in Fig. 4 the timing jitter normalized to its optimum value $\sigma_{\mathrm{t\_opt}}$ given in (22) for different pulse widths, considering both optical and

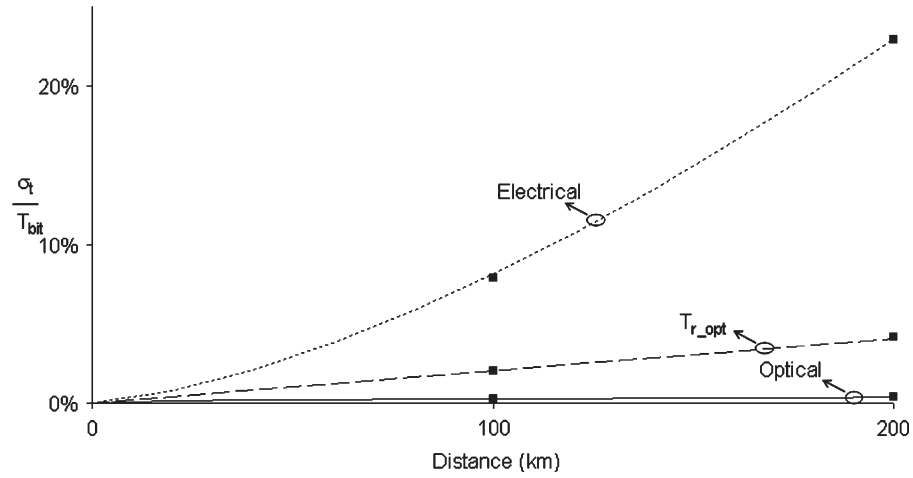

Fig. 3. Normalized timing jitter versus distance when a residual dispersion of 0.4 ps/nm/km is compensated electrically (short dashed curve). Considerable improvement can be realized when the pulse width is optimized for each distance (long dashed curve). The solid curve shows the case of full optical dispersion compensation. In each case, squares represent numerical results.

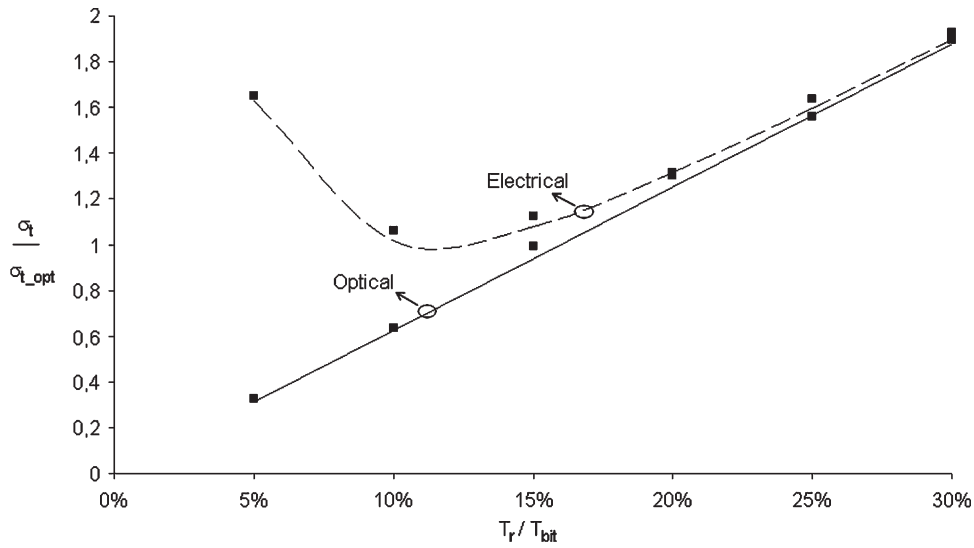

Fig. 4. Timing jitter normalized to its optimum value for different pulse widths for a 500-km-long system operating at 10 Gb/s. Square symbols represent numerical results.

electrical dispersion compensation. According to the results shown in Fig. 4, the optimum pulse width is around 11% of $T_{\rm bit}$ when electrical dispersion mitigation is employed, which agrees well with the value obtained directly from (21).

VII. Conclusion

In this work, we have considered timing jitter in a lightwave system in the absence of fiber nonlinearities. We use frequency-domain analysis and derive a new expression for the timing jitter after the photodetector. This expression shows that, when chromatic dispersion is fully compensated in the optical domain so that the pulse width at the receiver is fully recovered, the timing jitter is quite small because it grows only linearly with link length. In contrast, timing jitter grows with link length in a cubic fashion when dispersion is only partially compensated along the link, and the effects of residual dispersion are mitigated by means of electrical equalization.

We have also addressed the issue of optimum pulse width and how it can be used to reduce timing jitter. We show that there exists an optimum pulse width that minimizes the timing jitter due to ASE noise and chromatic dispersion. This optimum pulse width depends on the residual dispersion and on the link length. If we were to adjust the pulse width according to the transmission distance, we can attain a quadratic growth for the timing jitter even in the presence of residual dispersion.

The main conclusion of our work is that the cubic growth of timing jitter limits our ability to overcome chromatic dispersion electronically after photodetection. Our results imply that the best approach is to develop optical dispersion-compensation devices that can compensate the chromatic dispersion fully. At bit rates of 40 Gb/s or more that are planned for the near future, one must employ dynamic and tunable dispersion optical compensation to ensure that timing jitter is kept to a minimum after photodetection.

APPENDIX A
ACCUMULATED ASE NOISE AT THE END OF OPTICAL LINK

The accumulated ASE noise at the end of the optical link $N(\omega)$ is given by (10). Assuming that the noise generated in each amplifier is statistically independent of the noise generated in all other amplifiers, the average value and correlation of $N(\omega)$ are found to be, respectively

$$\begin{aligned}\overline{N(\omega)} &= \overline{\sum_{k=1}^{M} N_k(\omega) H(L-kL_A,\omega)} \\ &= \sum_{k=1}^{M} \overline{N_k(\omega)} H(L-kL_A,\omega) \\ &= 0 \end{aligned} \tag{26}$$

and

$$\begin{aligned}&\overline{N(\omega_1)N^*(\omega_2)} \\ &= \overline{\sum_{k=1}^{M} N_k(\omega_1) H(L-kL_A,\omega_1) \sum_{l=1}^{M} N_l^*(\omega_2) H^*(L-kL_A,\omega_2)} \\ &= \sum_{k=1}^{M}\sum_{l=1}^{M} \overline{N_k(\omega_1)N_l^*(\omega_2)} H(L-kL_A,\omega_1) H^*(L-kL_A,\omega_2) \\ &= \sum_{k=1}^{M} \overline{N_k(\omega_1)N_k^*(\omega_2)} H(L-kL_A,\omega_1) H^*(L-kL_A,\omega_2) \\ &= \sum_{k=1}^{M} \sigma_k^2 \delta(\omega_1-\omega_2) H(L-kL_A,\omega_1) H^*(L-kL_A,\omega_2) \\ &= M\sigma_k^2 \delta(\omega_1-\omega_2) \\ &= \frac{L}{L_A}\sigma_k^2 \delta(\omega_1-\omega_2) \\ &= \sigma^2 \delta(\omega_1-\omega_2). \end{aligned} \tag{27}$$

The effect of fiber dispersion on the kth amplifier noise $N_k(\omega)$ is to produce a frequency-dependent phase shift. The amount of this phase shift depends on the distance from the kth amplifier to the end of the system. It is obvious that this phase shift does not change the statistics of $N_k(\omega)$. Therefore, an alternative way to obtain (26) and (27) is to assume that the real and imaginary parts of $N(\omega)$ are the result of a sum of L/L_A statistically independent Gaussian random variables with zero mean and variance $\sigma_k^2/2$. Representing the real and imaginary parts of $N(\omega)$ by $R(\omega)$ and $I(\omega)$, and the real and imaginary parts of $N_k(\omega)$ by $R_k(\omega)$ and $I_k(\omega)$, we obtain

$$\overline{N(\omega)} = \overline{R(\omega)+iI(\omega)} = \frac{L}{L_A}\left[\overline{R_k(\omega)} + i\overline{I_k(\omega)}\right] = 0 \tag{28}$$

and

$$\begin{aligned}&\overline{N(\omega_1)N^*(\omega_2)} \\ &= \overline{[R(\omega_1)+iI(\omega_1)]\,[R(\omega_2)-iI(\omega_2)]} \\ &= \overline{R(\omega_1)R(\omega_2)+I(\omega_1)I(\omega_2)+iI(\omega_1)R(\omega_2)-iI(\omega_2)R(\omega_1)} \\ &= \frac{L}{L_A}\overline{R_k(\omega_1)R_k(\omega_2)} + \frac{L}{L_A}\overline{I_k(\omega_1)I_k(\omega_2)} \\ &= \frac{L}{L_A}\frac{\sigma_k^2}{2}\delta(\omega_1-\omega_2) + \frac{L}{L_A}\frac{\sigma_k^2}{2}\delta(\omega_1-\omega_2) \\ &= \frac{L}{L_A}\sigma_k^2\delta(\omega_1-\omega_2) \\ &= \sigma^2\delta(\omega_1-\omega_2). \end{aligned} \tag{29}$$

Taking into consideration that $R(\omega)$ and $I(\omega)$ are statistically independent random Gaussian variables with zero mean and variance given by $(L/L_A)(\sigma_k^2/2)$, and that they are also statistically independent of all other $R(\omega)$ and $I(\omega)$ at different frequencies, the following relations can be readily obtained, i.e.,

$$\overline{N^*(\omega)} = 0 \tag{30}$$

$$\overline{N(\omega_1)N(\omega_2)} = 0 \tag{31}$$

$$\overline{N^*(\omega_1)N^*(\omega_2)} = 0 \tag{32}$$

$$\overline{\frac{\partial N(\omega)}{\partial \omega}} = 0 \tag{33}$$

$$\overline{\frac{\partial N(\omega_1)}{\partial \omega_1}\frac{\partial N(\omega_2)}{\partial \omega_2}} = 0. \tag{34}$$

From (27), taking the derivative in order to ω_1, we obtain

$$\overline{\frac{\partial N(\omega_1)}{\partial \omega_1}N^*(\omega_2)} = \sigma^2\frac{\partial \delta(\omega_1-\omega_2)}{\partial \omega_1} \tag{35}$$

and in an analogous way

$$\overline{N^*(\omega_1)\frac{\partial N(\omega_2)}{\partial \omega_2}} = \sigma^2\frac{\partial \delta(\omega_2-\omega_1)}{\partial \omega_2}. \tag{36}$$

APPENDIX B
TIMING JITTER IN THE PRESENCE OF CHROMATIC DISPERSION AND NOISE

Here, we present a detailed derivation of the timing jitter expression given in Section IV. Replacing $U(z=L,\omega)$ by $S(L,\omega)+N(\omega)$ in (4), we obtain

$$\begin{aligned}t_p = &-\frac{i}{2\pi E_p}\int_{-\infty}^{+\infty}\left[S^*(L,\omega)\frac{\partial S(L,\omega)}{\partial \omega} + S^*(L,\omega)\frac{\partial N(\omega)}{\partial \omega}\right]d\omega \\ &-\frac{i}{2\pi E_p}\int_{-\infty}^{+\infty}\left[N^*(\omega)\frac{\partial S(L,\omega)}{\partial \omega} + N^*(\omega)\frac{\partial N(\omega)}{\partial \omega}\right]d\omega \end{aligned} \tag{37}$$

with

$$E_p = \frac{1}{2\pi}\int_{-\infty}^{+\infty} |S(L,\omega)|^2\, d\omega. \tag{38}$$

From (37), the average value of the pulse central position is given by

$$\begin{aligned}\overline{t_p} = &-\frac{i}{2\pi E_p}\overline{\int_{-\infty}^{+\infty} S^*(L,\omega)\frac{\partial S(L,\omega)}{\partial\omega}d\omega}\\ &-\frac{i}{2\pi E_p}\overline{\int_{-\infty}^{+\infty} S^*(L,\omega)\frac{\partial N(\omega)}{\partial\omega}d\omega}\\ &-\frac{i}{2\pi E_p}\overline{\int_{-\infty}^{+\infty} N^*(\omega)\frac{\partial S(L,\omega)}{\partial\omega}d\omega}\\ &-\frac{i}{2\pi E_p}\overline{\int_{-\infty}^{+\infty} N^*(\omega)\frac{\partial N(\omega)}{\partial\omega}d\omega}.\end{aligned} \tag{39}$$

Making use of (30) and (33), we readily obtain (15). From (37) and (15), we have

$$\begin{aligned}t_p - \overline{t_p} = &-\frac{i}{2\pi E_p}\int_{-\infty}^{+\infty} S^*(L,\omega)\frac{\partial N(\omega)}{\partial\omega}d\omega\\ &-\frac{i}{2\pi E_p}\int_{-\infty}^{+\infty} N^*(\omega)\frac{\partial S(L,\omega)}{\partial\omega}d\omega\\ &-\frac{i}{2\pi E_p}\int_{-\infty}^{+\infty} N^*(\omega)\frac{\partial N(\omega)}{\partial\omega}d\omega\\ &+\frac{i}{2\pi E_p}\int_{-\infty}^{+\infty}\overline{N^*(\omega)\frac{\partial N(\omega)}{\partial\omega}}d\omega.\end{aligned} \tag{40}$$

The third and forth terms that appear in (40) are due to the ASE–ASE beating, and their contribution tends to be much smaller than that of the first two terms if a narrowband optical filter is placed before the photodetector. In fact, the average in the fourth term is readily proved to be zero in view of (35). Keeping only the first two terms, the square of timing jitter is given by

$$\begin{aligned}(t_p - \overline{t_p})^2 = &-\frac{1}{4\pi^2 E_p^2}\int_{-\infty}^{+\infty}\int_{-\infty}^{+\infty} S^*(L,\omega_1)S^*(L,\omega_2)\\ &\times\frac{\partial N(\omega_1)}{\partial\omega_1}\frac{\partial N(\omega_2)}{\partial\omega_2}d\omega_1 d\omega_2\\ &-\frac{1}{4\pi^2 E_p^2}\int_{-\infty}^{+\infty}\int_{-\infty}^{+\infty}\frac{\partial S(L,\omega_1)}{\partial\omega_1}\frac{\partial S(L,\omega_2)}{\partial\omega_2}\\ &\times N^*(\omega_1)N^*(\omega_2)d\omega_1 d\omega_2\\ &-\frac{1}{4\pi^2 E_p^2}\int_{-\infty}^{+\infty}\int_{-\infty}^{+\infty} S^*(L,\omega_1)\\ &\times\frac{\partial S(L,\omega_2)}{\partial\omega_2}N^*(\omega_2)\frac{\partial N(\omega_1)}{\partial\omega_1}d\omega_1 d\omega_2\\ &-\frac{1}{4\pi^2 E_p^2}\int_{-\infty}^{+\infty}\int_{-\infty}^{+\infty} S^*(L,\omega_2)\frac{\partial S(L,\omega_1)}{\partial\omega_1}N^*(\omega_1)\\ &\times\frac{\partial N(\omega_2)}{\partial\omega_2}d\omega_1 d\omega_2.\end{aligned} \tag{41}$$

The variance of t_p is obtained by averaging (41). Making use of (32), (34), (35), and (36), we obtain

$$\begin{aligned}\sigma_t^2 = &\overline{(t-\overline{t_p})^2}\\ = &-\frac{1}{4\pi^2 E_p^2}\int_{-\infty}^{+\infty}\int_{-\infty}^{+\infty} S^*(L,\omega_1)\\ &\times\frac{\partial S(L,\omega_2)}{\partial\omega_2}\sigma^2\frac{\partial\delta(\omega_1-\omega_2)}{\partial\omega_1}d\omega_1 d\omega_2\\ &-\frac{1}{4\pi^2 E_p^2}\int_{-\infty}^{+\infty}\int_{-\infty}^{+\infty} S^*(L,\omega_2)\\ &\times\frac{\partial S(L,\omega_1)}{\partial\omega_1}\sigma^2\frac{\partial\delta(\omega_2-\omega_1)}{\partial\omega_2}d\omega_1 d\omega_2\\ = &-\frac{\sigma^2}{2\pi^2 E_p^2}\int_{-\infty}^{+\infty}\frac{\partial S(L,\omega_2)}{\partial\omega_2}\int_{-\infty}^{+\infty} S^*(L,\omega_1)\\ &\times\frac{\partial\delta(\omega_1-\omega_2)}{\partial\omega_1}d\omega_1 d\omega_2.\end{aligned} \tag{42}$$

Integrating by parts the integral over ω_1 and making use of Parseval's theorem, we obtain

$$\begin{aligned}\sigma_t^2 = &\frac{\sigma^2}{2\pi^2 E_p^2}\int_{-\infty}^{+\infty}\int_{-\infty}^{+\infty}\frac{\partial S(L,\omega_2)}{\partial\omega_2}\frac{\partial S^*(L,\omega_1)}{\partial\omega_1}\\ &\times\delta(\omega_1-\omega_2)d\omega_1 d\omega_2\\ = &\frac{\sigma^2}{2\pi^2 E_p^2}\int_{-\infty}^{+\infty}\left|\frac{\partial S(L,\omega)}{\partial\omega}\right|^2 d\omega\\ = &\frac{\sigma^2}{\pi E_p^2}\int_{-\infty}^{+\infty} t^2\,|s(L,t)|^2\, dt.\end{aligned} \tag{43}$$

Recalling the definition of the rms pulse width, this expression can be written in the simple form

$$\sigma_t^2 = \frac{\sigma^2}{\pi E_p}T_{\mathrm{r}}^2(L) \tag{44}$$

where T_{r} is the rms value of the pulse width at $z = L$, defined as in (17).

ACKNOWLEDGMENT

The authors acknowledge the suggestions of the reviewers.

REFERENCES

[1] G. P. Agrawal, *Fiber-Optic Communication Systems*, 3rd ed. Hoboken, NJ: Wiley, 2002.
[2] J. H. Winters and R. D. Gitlin, "Electrical signal processing techniques in long-haul fiber-optic systems," *IEEE Trans. Commun.*, vol. 38, no. 9, pp. 1439–1453, Sep. 1990.
[3] A. J. Weiss, "On the performance of electrical equalization in optical fiber transmission systems," *IEEE Photon. Technol. Lett.*, vol. 15, no. 9, pp. 1225–1227, Sep. 2003.
[4] C. R. S. Fludger, J. Whiteway, and P. Anslow, "Electronic equalization for low cost 10 gbit/s directly modulated systems," presented at the Optical Fiber Communication (OFC), Los Angeles, CA, 2004, Paper WM7.
[5] V. Curri, R. Gaudino, A. Napoli, and P. Poggiolini, "Electronic equalization for advanced modulation formats in dispersion-limited systems," *IEEE Photon. Technol. Lett.*, vol. 16, no. 11, pp. 2556–2557, Nov. 2004.
[6] J. P. Gordon and H. A. Haus, "Random walk of coherently amplified solitons in optical fibers," *Opt. Lett.*, vol. 11, no. 10, pp. 665–667, 1986.
[7] V. S. Grigoryan, C. R. Menyuk, and R. M. Mu, "Calculation of timing and amplitude jitter in dispersion-managed optical fiber communications using linearization," *J. Lightw. Technol.*, vol. 17, no. 8, pp. 1347–1356, Aug. 1999.
[8] J. Santhanam, C. J. McKinstrie, T. I. Lakoba, and G. P. Agrawal, "Effects of precompensation and post-compensation on timing jitter in dispersion-managed systems," *Opt. Lett.*, vol. 26, no. 15, pp. 1131–1133, Aug. 2001.
[9] C. J. McKinstrie, J. Santhanam, and G. P. Agrawal, "Gordon–Haus timing jitter in dispersion-managed systems with lumped amplification: Analytical approach," *J. Opt. Soc. Amer. B, Opt. Phys.*, vol. 19, no. 4, pp. 640–649, Apr. 2002.
[10] E. Poutrina and G. P. Agrawal, "Timing jitter in dispersion-managed soliton systems with distributed, lumped, and hybrid amplification," *J. Lightw. Technol.*, vol. 20, no. 5, pp. 790–797, May 2002.
[11] P. Monteiro, A. Borjak, J. da Rocha, J. O'Reilly, and I. Darwazeh, "Adjustable post-detection filters for optically amplified soliton systems," *IEICE Trans. Electron.*, vol. E85-C, no. 3, pp. 511–518, Mar. 2002.
[12] D. Marcuse, "RMS width of pulses in nonlinear dispersive fibers," *J. Lightw. Technol.*, vol. 10, no. 1, pp. 17–21, Jan. 1992.
[13] A. Papoulis, *The Fourier Integral and Its Applications*. New York: McGraw-Hill, 1962.
[14] A. N. Pinto, G. P. Agrawal, and J. F. da Rocha, "Effect of soliton interaction on timing jitter in communication systems," *J. Lightw. Technol.*, vol. 16, no. 4, pp. 515–519, Apr. 1998.
[15] E. Desurvire, *Erbium-Doped Fiber Amplifiers*. New York: Wiley, 1994.
[16] J. Goodman, *Statistical Optics*. New York: Wiley, 1985.
[17] J. P. Gordon and L. F. Mollenauer, "Effects of fiber nonlinearities and amplifier spacing on ultra-long distance transmission," *J. Lightw. Technol.*, vol. 9, no. 2, pp. 170–173, Feb. 1991.
[18] H. Ereifej, R. Holzlöhner, G. Carter, and C. Menyuk, "Intersymbol interference and timing jitter measurements in a 40-Gb/s long-haul dispersion-managed soliton system," *IEEE Photon. Technol. Lett.*, vol. 14, no. 3, pp. 343–345, Mar. 2002.

Armando Nolasco Pinto (M'00) was born in Oliveira do Bairro, Portugal, on 1971. He graduated with a degree in electronic and telecommunications engineering and received the Ph.D. degree in electrical engineering, both from the University of Aveiro, Aveiro, Portugal, in 1994 and 1999, respectively.

He is currently an Assistant Professor at the Electrical and Telecommunications Department, University of Aveiro, and a Researcher at the Institute of Telecommunications, Aveiro. He is the author and/or coauthor of more than 60 research papers. His main research interests focus on optical communication systems, mainly in nonlinear, polarization, and temperature-dependent effects in fibers optics.

Dr. Pinto is a member of the Optical Society of America (OSA).

José R. Ferreira da Rocha (M'90) was born in Mozambique, Africa. He received the M.Sc. degree in telecommunication systems and the Ph.D. in electrical engineering, both from the University of Essex, Essex, U.K., in 1980 and 1983, respectively.

He participates actively in the Telecommunications Institute, a national R&D nonprofit organization where he is a member of the Management Committee (Aveiro branch) and the National Coordinator for the Optical Communications Area. He has coordinated the University of Aveiro, Aveiro, Portugal, and Telecommunications Institute participation in various projects included in the following European Union (EU) R&D Programs in the area of telecommunications: RACE, RACE II, ACTS, and IST. In the past few years, he has acted as a Technical Auditor, Evaluator, and Independent Observer for the evaluation of projects submitted to various EU R&D Programs. He has also participated in various project evaluation boards set up by the Engineering and Physical Sciences Research Council (EPSRC), United Kingdom. By invitation of the ACTS Management Committee, he participated in the "Expert Groups on Visionary Research in Communications," aiming to create a bridge between the activities carried out in the Fourth and the Fifth Framework Programs on EU activities in the field of research, technological development, and demonstration. He is currently a Full Professor at the University of Aveiro. He has published about 170 papers, mainly in international journals and conferences. His present research interests include modulation formats and receiver design for very high capacity (above 40 Gb/s) optical communication systems based on linear and nonlinear transmission and wavelength division multiplexing (WDM) optical networks.

Qiang Lin received the B.S. degree in applied physics and the M.S. degree in optics, both from Tsinghua University, Beijing, China, in 1996 and 1999, respectively, and is currently working toward the Ph.D. degree at the Institute of Optics, University of Rochester, Rochester, NY.

His research interest includes nonlinear fiber optics, polarization mode dispersion, optical communications, and ultrafast optics.

Govind P. Agrawal (M'83–SM'86–F'96) received the B.S. degree from the University of Lucknow, New Delhi, India, in 1969, and the M.S. and Ph.D. degrees in Physics from the Indian Institute of Technology, New Delhi, in 1971 and 1974, respectively.

After holding positions at Ecole Polytechnique, France, the City University of New York, and AT&T Bell Laboratories, Murray Hill, NJ, he joined in 1989 the Faculty of the Institute of Optics, University of Rochester, Rochester, NY, where he is a Professor of Optics. He is the author and/or coauthor of more than 300 research papers, several book chapters and review articles, and seven books entitled *Semiconductor Lasers* (Norwell, MA: Kluwer, 2nd ed., 1993), *Fiber-Optic Communication Systems* (New York: Wiley, 3rd ed., 2002), *Nonlinear Fiber Optics* (San Diego, CA: Academic, 3rd ed., 2001), *Applications of Nonlinear Fiber Optics* (San Diego, CA: Academic, 2001), *Optical Solitons: From Fibers to Photonic Crystals* (San Diego, CA: Academic Press, 2003), *Lightwave Technology: Components and Devices* (Hoboken, NJ: Wiley, 2004), and *Lightwave Technology: Telecommunication Systems* (Hoboken, NJ: Wiley, 2005). He has participated numerous times in organizing technical conferences sponsored by the Optical Society of America (OSA) and IEEE. His research interests focus on optical communications, nonlinear optics, and laser physics.

Dr. Agrawal is a fellow of the OSA. He was the Program Cochair in 1999 and the General Cochair in 2001 for the Quantum Electronics and Laser Science Conference. He was a member of the Program Committee in 2004 and 2005 for the Conference on Lasers and Electro-Optics (CLEO).